EFFECTS OF TRANSPORT DELAYS ON MANUAL CONTROL SYSTEM PERFORMANCE

R. Wade Allen
Richard J. DiMarco

Systems Technology, Inc.
13766 S. Hawthorne Blvd.
Hawthorne, CA 90250

Telephone No. 213/679-2281

ABSTRACT

Throughput or transport delays in manual control systems can cause degraded performance and lead to potentially unstable operation. With the expanding use of digital processors, throughput delays can occur in manual control systems in a variety of ways such as in digital flight control systems in real aircraft, and in equation-of-motion computers and CGI's in simulators. Previous research has shown the degrading effect of throughput delays on subjective opinion and system performance and dynamic response. A generic manual control system model is used in this paper to provide a relatively simple analysis of and explanation for the effects of various types of delays. The consequences of throughput delays of some simple system architectures is also discussed.

A. OVERVIEW AND BACKGROUND

Past literature surveys associated with flight simulation fidelity have found that system response lags and computational delays cause performance and pilot subjective rating problems (Refs. 1 and 2). Pilot/vehicle model analysis has shown that delays on the order of 50 to 100 msec can have an appreciable influence on performance and workload (Ref. 3). Recent experiments have shown performance effects of time delays which are consistent with model analysis (Refs. 4 and 5).

The above literature indicates that simulator computational delays can have a serious effect on aircraft simulation fidelity. Ground vehicles typically have faster response dynamics than aircraft in terms of path control, and it is suspected that the problem may be even more serious for driving simulators. To further understand the effect of various potential sources of transport delays a computer model analysis was undertaken using a generic vehicle control model as described below. The analysis was carried out to study the effect of several sources of computational delay including host computer system, display system, and motion system. (This analysis does not address another important simulation artifact, that of the mismatch between visual and motion cues, which can lead to vertigo and/or sickness.)

B. ANALYSIS MODEL

The basic control example for the analysis model concerns generic vehicle tracking (e.g., dogfighting) where the operator must point his vehicle at a target or aim point at some fixed distance in front of the vehicle. An example for a typical aircraft is shown in Fig. 1 (Ref. 6). A similar arrangement holds for ground vehicle steering control as illustrated in Fig. 2 (Ref. 7). The only dynamic difference between the car and aircraft examples is the T_{θ_2} path lag which is ignored for the car. (It actually exists in the car, but as a very high frequency lag corresponding to an aircraft with steep lift or side-force curve slopes.)

A generic operator/vehicle pointing control model was prepared for analysis based on an expansion of the Figs. 1 and 2 models. A block diagram of the analysis model is shown in Fig. 3 which has additional dynamic complexity over the simplified models of Figs. 1 and 2 as follows:

- Pilot lead generation to compensate for effective vehicle lag, T_{eq}, is provided by angular rate feedback which is assumed to represent a composite of motion perception (i.e., acceleration, angular rotation and proprioceptive sensations).
- Lightly damped, second-order limb/manipulator dynamics.
- Human operator transport delay associated with visual (τ_v) and motion (τ_r) perception.
- System transport delays associated with dynamic computations (τ_c), display generation (τ_d), and motion feedback (τ_m).
- A low frequency trimming operation to minimize low frequency "hang off" errors.

In the Fig. 3 analysis model, a disturbance (δ_d) is added at the input to the equivalent vehicle dynamics to represent the effects of wind gusts, and roadway inputs in the case of ground vehicles. The equivalent vehicle dynamics are represented by s simple first-order time constant, T_{eq}, to approximate lags in vehicle rotational rate in response to control inputs. Path lag, T_{θ_2}, is assumed to be zero for this analysis. Transport delay representations are defined below.

C. TRANSPORT DELAY SOURCES

The model analysis was arranged to assess the effects of three sources of computational delay. The first is a transport delay associated with the vehicle dynamics equations of motion (τ_c). This delay could represent the equivalent delay used in specifying vehicle handling qualities (Ref. 8) which can result from the composite effect of stick filters, digital flight control system delays, and control system and other high frequency vehicle dynamics effects. It could also represent the composite effect of A/D and D/A sampling holds, integration routines and computational cycle time. The analysis considered either no delay, which might correspond to an analog vehicle or an

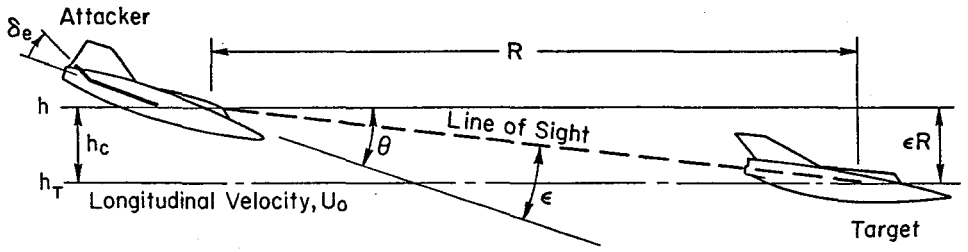

a) Model Scenario

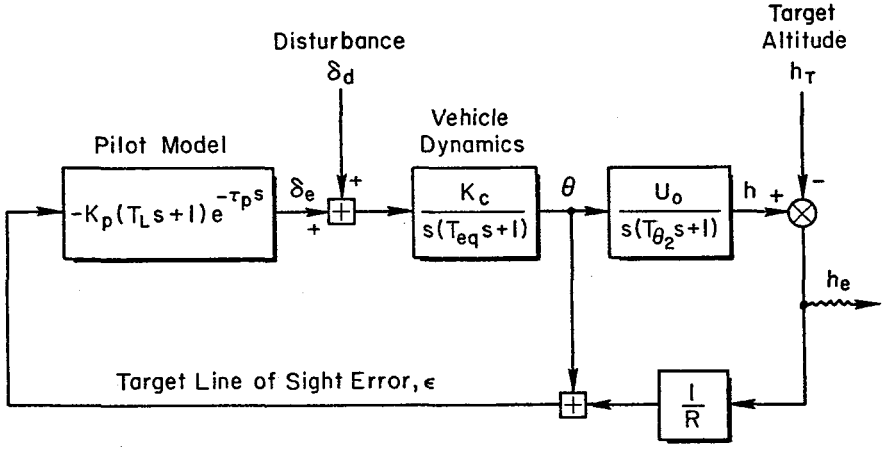

b) Pilot-Aircraft System Dynamics

Figure 1. System Model for Air-to-Air Target Tracking

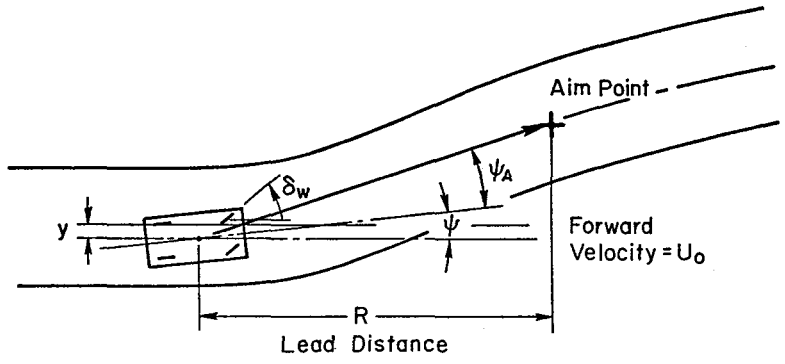

a) Model Scenario

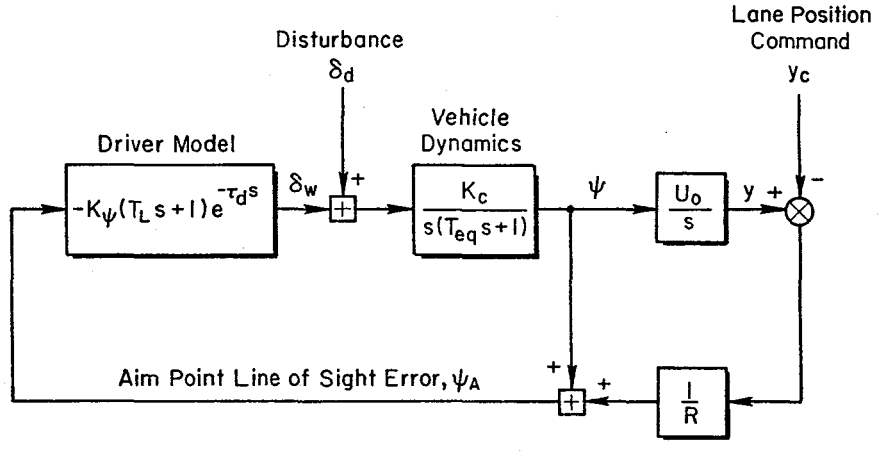

b) Driver-Automobile System Dynamics

Figure 2. System Model for Car/Driver Path Following a Commanded Path

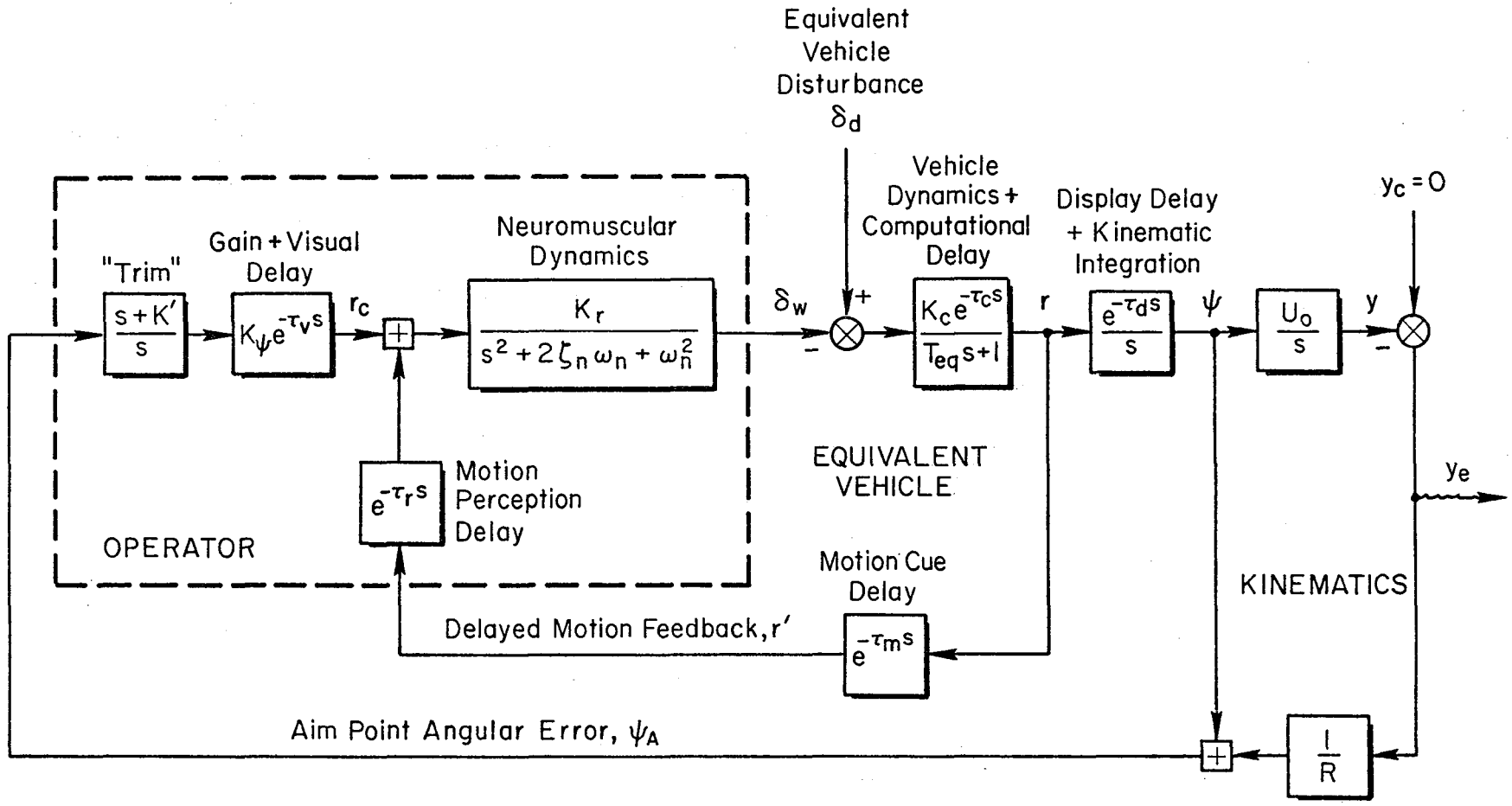

Figure 3. Generic Operator/Vehicle Tracking Dynamic Model for Analyzing Transport Delay Effects

analog simulation computer, or a delay of 0.075 sec, which is a common equivalent delay time associated with complicated digital simulation computations or modern high performance aircraft with digital flight control systems.

The second delay source considered was that due to display system characteristics. Analysis conditions included either no delay, which might be associated with an analog processor, or 100 msec delay which is common to many of the current generation simulation CGI raster scan devices. The delay time condition might also be associated with the camera servos on a terrain board system, or digital processing in HUD or EADI instruments.

The final delay factor was concerned with motion feedback to the human operator. Analysis conditions included no delay, or a rather long delay of 250 msec. The long-delay condition might be associated with a fixed-based simulator environment where there were no motion cues available, and the human operator has to generate heading rate cues visually. This could also result from motion lags in a simulator motion system combined with computational delay in generating the motion base drive commands. The additional 250 msec was calculated to give model behavior that was consistent with past measurements made under both fixed-based and moving base conditions (Ref. 9), and is also consistent with delays identified in flight simulators (Ref. 10).

D. MODEL PARAMETER SELECTION

The Fig. 3 model has a variety of parameters that must be set to represent either vehicle characteristics or human operator behavior. A nominal vehicle heading time constant (T_{eq}) of about 0.2 sec was selected. This might represent a light weight, high performance aircraft, or a compact to intermediate size automobile. The vehicle gain is somewhat arbitrary, depending both on control gain and vehicle stability derivatives.

The human operator model parameters can be divided into two groups; those which are relatively fixed and were assumed to be constant for this analysis, and other parameters which the human operator typically adapts in order to achieve stable and desirable closed-loop performance. The trim constant (K') was assumed to be constant at 0.5 rad/sec which is consistent with driver measurements discussed in Ref. 7. The visual time delay (τ_v) was assumed to be constant at 0.05 sec. The time delay associated with motion feedback perception (τ_r) was also set at 0.05 sec. The second-order limb/manipulator system dynamics were set at a break frequency of 20 rad/sec and a damping ratio of 0.5. The pure delay and lag characteristic were set to give a composite effective time delay, with the motion feedback loop closed, of 0.17 seconds which is consistent with past car-driver measurements (Ref. 7).

The human operator can arbitrarily adapt his inner and outer loop gains (K_r and K_ψ respectively) and has some control over aim point range, R, to optimize system performance and control stability. For the model structure assumed here, K_r was adjusted to obtain as wide a frequency response as possible in the motion feedback loop while maintaining a reasonable closed-loop damping ratio (i.e., $\zeta_{CL} \cong 0.5$). For a real vehicle without any computer delay or extra motion feedback delays the variable K_r would be adjusted to

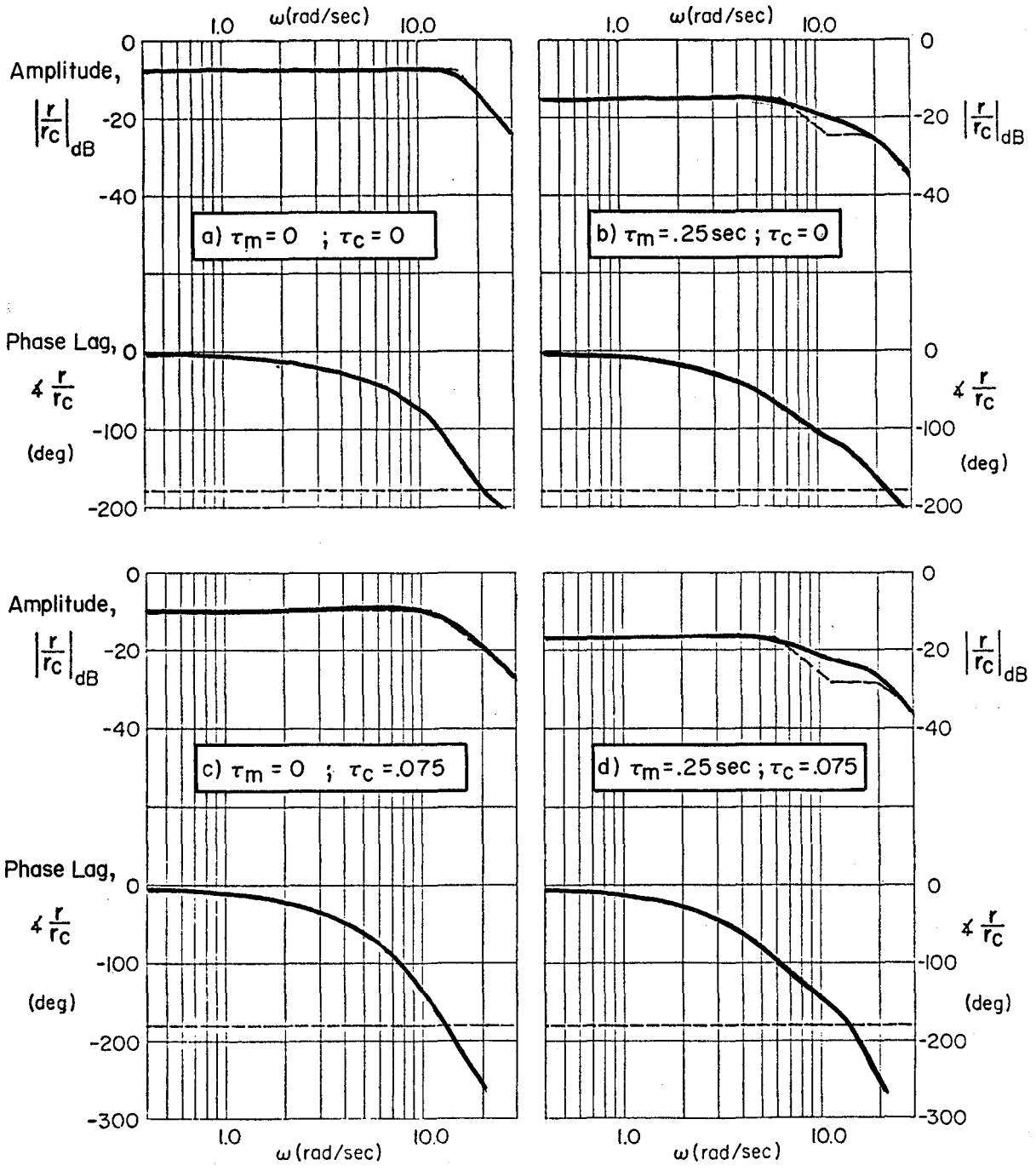

Figure 4. Motion Feedback Closed-Loop Response Functions (Equivalent Closed-Loop Parameters Given in Table 1)

TABLE 1. MOTION FEEDBACK LOOP PARAMETERS FOR VARIOUS LEVELS OF MOTION FEEDBACK (τ_m) AND COMPUTATIONAL (τ_c) DELAY

OPEN LOOP			EQUIVALENT CLOSED	
τ_m (sec)	τ_c (sec)	K_{r-1} (sec^{-1})	K_{eq} (sec)	τ_o (sec)
0	0	500	0.414	0.12
	0.075	350	0.331	0.20
0.25	0	150	0.175	0.16
	0.075	125	0.150	0.235

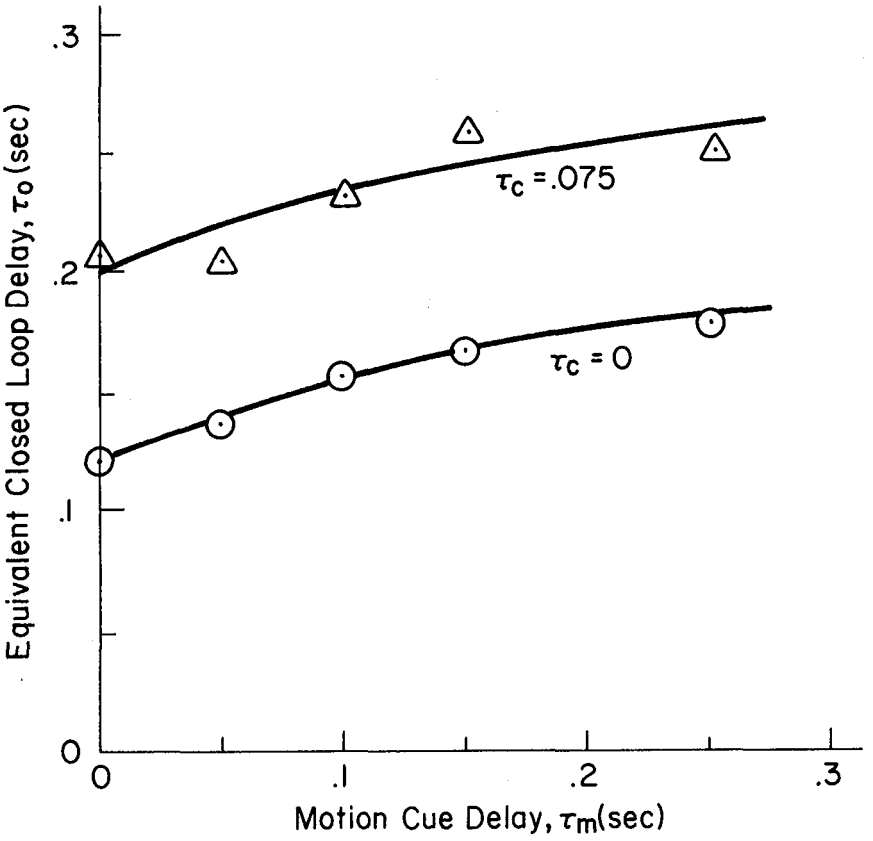

Figure 5. Equivalent Motion Feedback Delay for Various Levels of τ_m and τ_c

cancel out the effects of the vehicle equivalent heading lag, T_{eq}. As computational delay is added or the heading rate feedback delay is changed, K_r would then be adjusted to still achieve as wide a bandwidth as possible with this inner loop.

When K_r is properly adjusted a fairly flat closed-loop amplitude ratio can be achieved for the motion feedback loop as illustrated in Fig. 4. When the conditions in Fig. 4 are achieved the closed-loop response of the motion feedback loop can then be approximated by a gain and an equivalent time delay up to the point where the amplitude ratio begins to roll off:

$$\text{Motion Feedback Closed-Loop Response} \cong K_{eq}e^{-\tau_o}$$

Closed-loop equivalent parameters are given in Table 1 for the Fig. 4 response functions.

Note that when there are no extra computational delays and a low feedback delay, as in the upper lefthand corner of Fig. 4, the closed-loop bandwidth of the heading rate loop can be adjusted to be quite high. Theoretically, in this case the bandwidth is on the order of 15 rad/sec, and the equivalent time delay is quite small (about 120 msec). If τ_o is added to the visual time delay (τ_v), the result is an overall equivalent time delay for the driver of about 0.17 sec, which is consistent with measurements discussed in Ref. 7. On the other hand, when a significant amount of delay is put into the motion feedback loop, as in the lower righthand corner of Fig. 4, the closed-loop bandwidth of the heading rate loop is reduced considerably. In this case it is reduced to the vicinity of the vehicle's heading rate time constant (i.e., delayed feedback effectively opens the loop). In the second case the equivalent time delay for the heading rate loop is increased to about 235 msec.

E. EQUIVALENT OPERATOR/VEHICLE TIME DELAY EFFECTS

The equivalent closed-loop time delays that are achieved over a wide range of motion feedback delays (τ_m) and two levels of computational delay are illustrated in Fig. 5. Here, note that the computer computation delay (τ_c) has a much greater influence on the equivalent closed-loop delay than does the motion feedback time delay which is actually in the feedback of this loop. These induced delays will have two effects on human operator/vehicle performance. First, the increased equivalent closed-loop time delay will affect the operator's ability to achieve an overall bandwidth in controlling outer loop errors. Second, the effect of disturbances that act on the vehicle will be delayed in their feedback to the operator. Thus, there will be an overall delay in the human operator responding to a disturbance, and, once the operator responds, he will be limited in the bandwidth of his response.

The parameters that remain to be selected in the Fig. 3 model are K_ψ and U_o/R. Procedures for optimizing human operator performance by the selection of these two variables has been discussed for car driving in Ref. 7. The procedure involves breaking the Fig. 3 model loop at the r_c point and then considering the composite driver/vehicle open-loop transfer function proceeding around the loop.

Given that the inner loop closed-loop dynamics can be interpreted as an equivalent time delay over the outer loop bandwidth, then an Extended Crossover Model describing function for the Fig. 3 model can be written as:

$$Y_p{}^*Y_c = \underbrace{\frac{s + K'}{s}}_{\text{Low Frequency Trimming}} \cdot \underbrace{\frac{s + U_o/R}{s}}_{\text{Low Frequency Kinematic Lead + Integration}} \cdot \underbrace{\frac{\omega_c e^{-\tau_e s}}{s}}_{\text{Crossover Model}} \qquad (1)$$

The kinematic zero at U_o/R is at low enough frequency that the dynamics become K/s-like in the region of magnitude crossover (the classical crossover model law). Now the optimum K_ψ and U_o/R values can be interpreted in terms of crossover frequency and phase margin.

The $Y_p{}^*Y_c$ transfer function is illustrated in Fig. 6 for each combination of induced time delays under consideration. As noted in Fig. 6, the low frequency effects of aim point kinematics $(s + (U_o/R))/s$ plus trimming $(s + K')/s$ have resulted in a conditionally stable system. The variable U_o/R which corresponds to lead distance or look-ahead range for the human operator's aim point was adjusted to give the stable phase region indicated in Fig. 6. As can be noted, U_o/R was varied for each combination of the various time delays in Fig. 6 in order to get a similar stable phase region for all conditions. Once this form had been achieved, then the remaining variable K_ψ was selected in order to give a specified phase margin. The low frequency kinematic and trim effects cause a significant reduction in phase margin in the crossover frequency region and cannot be neglected for tasks requiring control to aim points with speed-to-range ratios in the region of 0.1-1.0 rad/sec. It should be noted that situations which constrain the look ahead distance R to small values (e.g., driving in the fog, pointing at short range ground or air targets) could decrease the region over which the phase is stable.

Phase margin has been used previously as a metric for quantifying the stability of car/driver closed-loop steering performance (Ref. 11). K_ψ is set to achieve a desired phase margin at the crossover frequency which can be considered the bandwidth of the closed-loop operator/vehicle control system. The phase margin quantifies the stability or oscillatory nature of the operator's steering control behavior. The bandwidth or crossover frequency defines how rapidly the control can be carried out. For this analysis an attempt was made to maintain a constant phase margin of 30 deg for all cases. This level has been typically found in past car driving studies (Ref. 7). The achievable crossover frequency depends on the total system time delay which includes the inner loop equivalent time delay, visual perceptual delay, and display system transport delay:

$$\tau_e = \tau_o + \tau_v + \tau_d$$

Gain and crossover model parameters are summarized in Table 2.

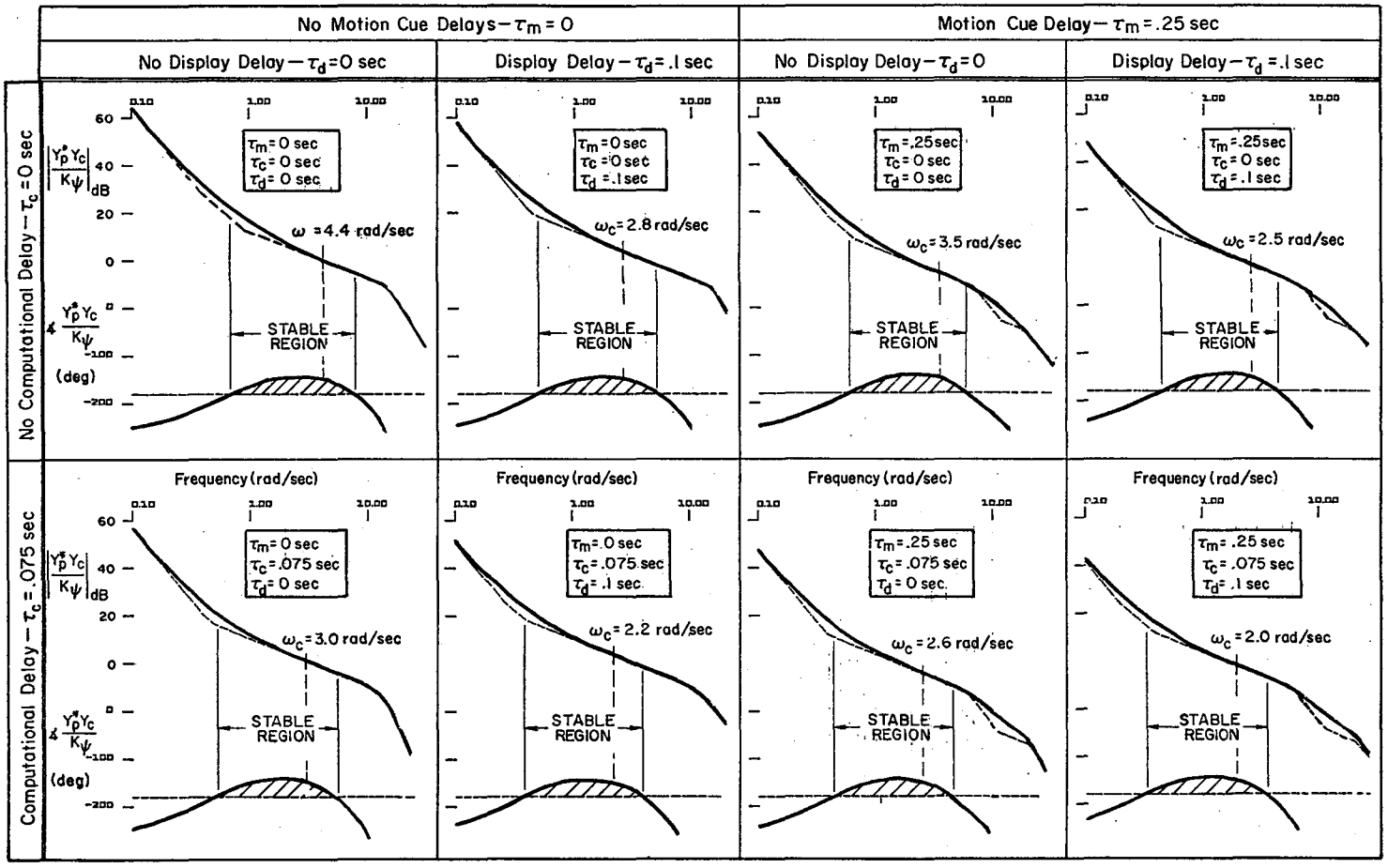

Figure 6. Equivalent Open-Loop Human Operator/Vehicle Describing Functions For Various Levels of Simulation Time Delays

TABLE 2. HUMAN OPERATOR/VEHICLE GAIN AND CROSSOVER MODEL PARAMETERS FOR VARIOUS COMBINATIONS OF INDUCED VEHICLE/SIMULATOR DELAYS

VEHICLE/SIMULATOR INDUCED DELAYS			GAINS		CROSSOVER MODEL PARAMETERS	
τ_m (sec)	τ_c (sec)	τ_d (sec)	U_o/R (rad/sec)	K_ψ (sec^{-1})	ω_c (rad/sec)	τ_e (sec)
0	0	0	0.92	10.26	4.4	0.17
		0.1 sec	0.44	6.59	2.8	0.27
	0.075 sec	0	0.50	8.60	3.0	0.25
		0.1 sec	0.26	6.39	2.2	0.345
0.25 sec	0	0	0.65	18.51	3.5	0.215
		0.1 sec	0.35	13.47	2.5	0.305
	0.075 sec	0	0.38	16.13	2.6	0.29
		0.1 sec	0.20	12.58	2.0	0.38

F. BANDWIDTH EFFECTS

The consequences of the above adjustment procedures can be seen in Fig. 7. Here observe that the control bandwidth of the operator/vehicle system drops dramatically as various delays are added into the simulation loop. Adding the 0.1 sec display delay has the largest single impact on equivalent time delay and system bandwidth. Motion cue delays had the least impact. Computational delays had an effect somewhere in between motion cue delays and display delays. Perhaps if the computational delay had been 100 msec it would have had a similar effect to the display delay. The concatenation of these various delay sources deteriorates the system bandwidth to an even greater degree. When all the delay sources were combined, the system bandwidth was cut by more than 50 percent.

The relationship shown in Fig. 7 is a consequence of maintaining a constant phase margin. If we had changed the desired phase margin, or chosen a different aim point range (thus changing the low frequency kinematic root U_o/R) then a different constant would have resulted. In any case, we can use the hyperbolic relationship between ω_c and τ_e to determine how changes in effective system time delay affect achieveable bandwidth. Assume that a 25 percent decrease in system bandwidth is permissable. Then

$$\frac{\omega_c'}{\omega_c} = 0.75 = \frac{K/\tau_e'}{K/\tau_e} \rightarrow \tau_e' = \frac{\tau_e}{0.75}$$

or

$$\tau_e' - \tau_e = \Delta\tau_e = \frac{1}{3}\tau_e$$

Thus, an increase of one third in the total effective system time delay (τ_e) would be acceptable. For exceptionally responsive real world systems, such as cars which can result in effective time delays on the order of 0.17 seconds (Ref. 7), such an incremental increase in time delay due to simulator characteristics, would be on the order of 50 msec. (Maximum time delays on the order of 40 msec have previously been recommended for driving simulators, Ref. 12.) For sluggish real world systems where effective system time delays might be 0.3-0.4 seconds, then incremental time delays on the order of 100 msec might be acceptable.

Regardless of the value of the constant in the Fig. 7 relationship, the tradeoff between system bandwidth and effective system time delay is fundamental, and gives some insight into the consequences of added computational delays, whatever their origin.

G. PERFORMANCE EFFECTS

A δ_d impulse disturbance was applied to the Fig. 3 model as indicated in order to investigate the performance consequences of various time delay sources. The impulse input might be attributable to a wind gust or road input

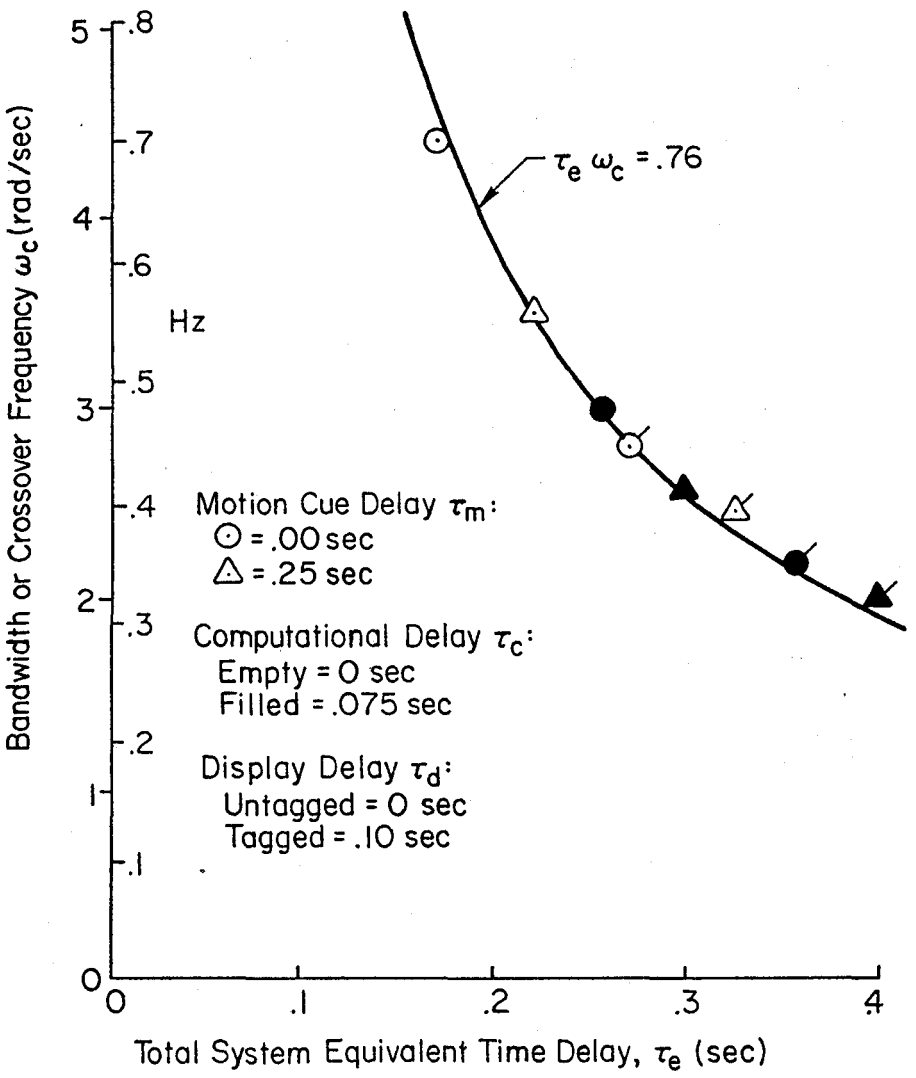

Figure 7. System Bandwidth as a Function of System Time Delay

in the case of ground vehicles. Time histories of the model transient response to an impulse disturbance input are illustrated in Fig. 8 for an automobile traveling at U_o = 80 ft/sec (55 mph). For the low frequency kinematic characteristics given in Table 2 (U_o/R = 0.2-0.92) the Fig. 8 transients could also be scaled to represent airplane motions in the Fig. 1 model (e.g., at 800 ft/sec this would represent target ranges of roughly 900-4000 ft).

The effects of the various transport delays on system performance are quite evident in Fig. 8. Note that the model's ability to maintain lane position deteriorates radically as the amount of simulator delay is increased. The effect of the various delay sources are directly observable in the steering wheel response of the model driver. As the delay sources are concatenated, the model driver takes longer and longer to initially respond to the input disturbance. This is consistent with the data given in Table 2 which shows the total effective system time delay increasing from a no delay level of 0.17 seconds to 0.38 seconds in the worst delay case.

The cycle time of the system transient response also obviously increases with increasing delay sources in Fig. 8. This effect is consistent with the decreasing bandwidth as a function of time delay shown in Fig. 7. Because of the driver/vehicle system's increasingly delayed regulatory response to the transient input, the maximum vehicle heading deviation nearly doubles in the worst delay case compared to the no delay condition, and the lane deviation increases by more than a factor of three with the increasing delay. Note also that each of the delay components considered separately in Fig. 8 have a similar effect on system performance, as does the concatenation of any two delay sources.

H. SYSTEM ARCHITECTURE AND DELAY COMPENSATION

The effective system delays analyzed herein can arise from a variety of sources. Effective computational delays are due to a composite of A/D and D/A operations, computational algorithms (e.g., integration routines) and general software architecture. Cycle time may not be a true measure of effective delay if some routines are updated more often than others (e.g., high frequency modes might be updated more rapidly than kinematic integrations). Motion drive computations can have analogous considerations, and the frequency response of the drive servos must also be accounted for. CGI systems must maintain high refresh and update rates to portray smooth motion (i.e., typically 50 Hz or above), but multiple frame times may be required for angular and translational commands work their way through typical pipeline architectures.

Delay compensation can be considered at various stages in the system architecture. Minimum delay integration routines should be considered for dynamic computations (Ref. 13). The update of motion and angular orientation cues are more critical to closed-loop operator/vehicle system response than outer loop translational information that is already delayed by kinematic integration. Thus in computing equations of motion, angular rates and orientation, and accelerations could be updated more rapidly than inertial velocity and position. In CGI display systems, angular transformations could be updated more rapidly than perspective transformations.

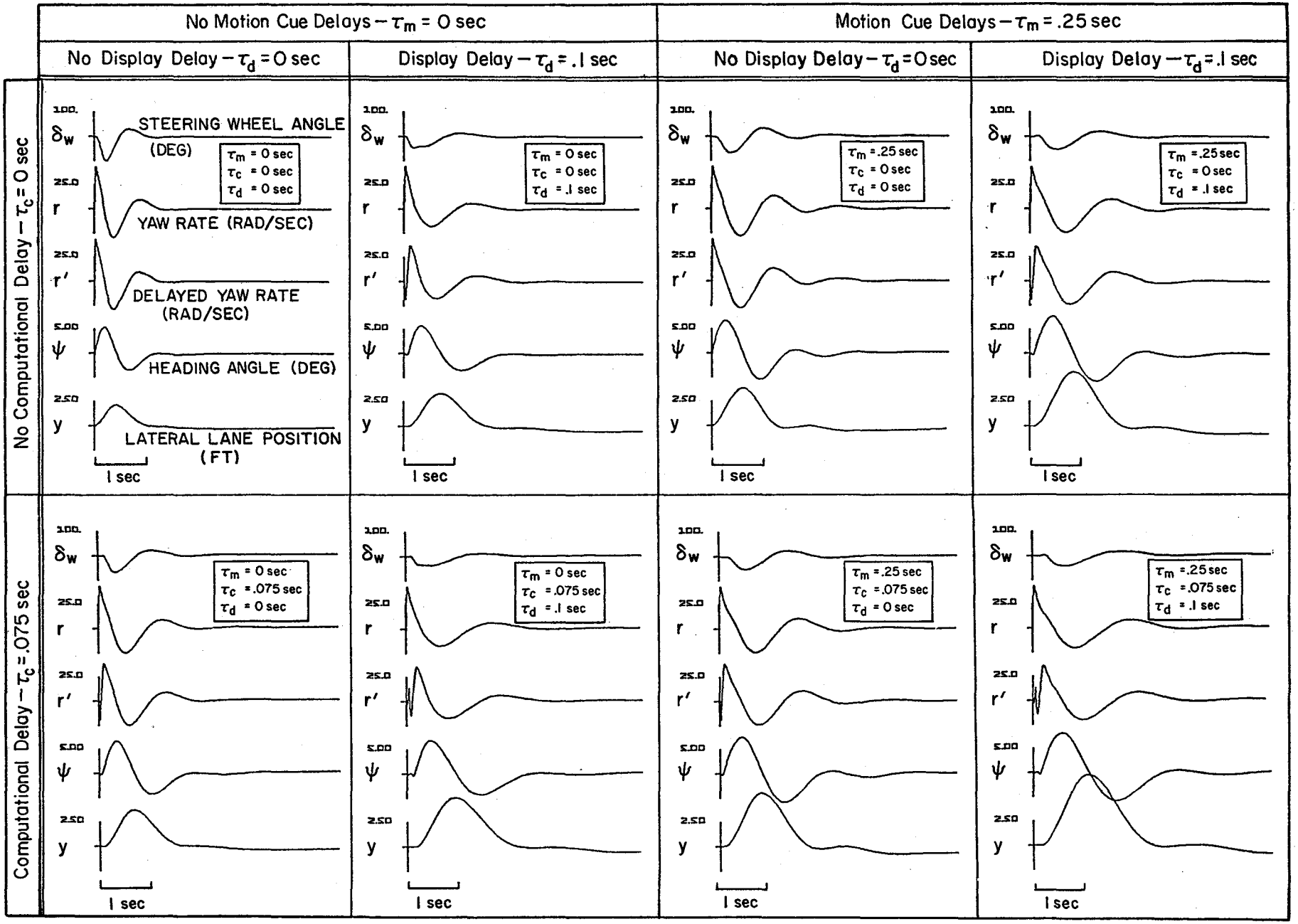

Figure 8. Driver/Vehicle System Closed-Loop Response to an Impulse Disturbance

Lead or rate compensation might be considered for both host computer and CGI computations. Overall system dynamics should be considered here, however. The transfer functions in Figs. 4 and 6 suggest that for systems with adequate motion cues, lead frequencies in the region of the human operators limb/manipulator bandwidth (> 10 rad/sec) might be acceptable, while in the case of delayed or no motion cues, lead compensation could be increased to cover the bandwidth above the basic vehicle dynamics bandwidth. In general lead frequency must be above system crossover frequency (ω_c) in orcer to avoid compromising system gain margin.

I. CONCLUDING REMARKS

The model analysis herein shows that the effects of several computational delay sources in manual vehicle control systems can be evaluated to a first approximation by their effect on a composite effective system time delay. This effective time delay constrains the closed-loop bandwidth that can be achieved by the human operators. Tolerable computational delays can be determined by specifying a permissable system bandwidth reduction. The model analysis also shows that degradation in performance, such as regulation against transient disturbance, is consistent with system bandwidth reduction.

In general, compensation for effective system delays must be considered in an overall system context. System delays and compensation effects should be measured with input/output identification procedures using appropriate system inputs and sensors to measure outputs (e.g., gyros and accelerometers to measure platform motions and photo detectors to measure display system response). Response functions should be compensated to approach the less delayed response of the ideal target system. Finally, the fidelity of the system response should be considered from the human operator's point of view. In moving base systems, visual and motion cues should be consistent, and in general perceived vehicle response should be consistent with the operator's expectations. The analytic consequences of these fidelity considerations are not well understood, and typically would require final empirical tuneup.

REFERENCES

1. Puig, Joseph A., William T. Harris, and Gilbert L. Ricard, Motion in Flight Simulation: An Annotated Bibliography, NAVTRAEQUIPCEN IH-298, July 1978.

2. Semple, Clarence A., Robert T. Hennessy, Mark S. Sanders, et al., Aircrew Training Device Fidelity Features, AFHRL-TR-80-36, Feb. 1980.

3. Baron, Sheldon, Ramal Muralidharan, and David Kleinman, "Closed Loop Models for Analyzing the Effects of Simulator Characteristics," AIAA Paper 78-1592, presented at the AIAA Flight Simulation Technologies Conference, Arlington, TX, 18-20 Sept. 1978, pp. 138-148.

4. Parrish, Russell V., Burnell T. McKissick, and Billy R. Ashworth, "Comparison of Simulator Fidelity Model Predictions with In-Simulator Evaluation Data," NASA TP-2106, Feb. 1983.

5. Hess, Ronald A., "The Effects of Time Delays on Systems Subject to Manual Control," AIAA Paper 82-1523, presented at the AIAA Guidance and Control Conference Proceedings, San Diego, CA, 9-11 Aug. 1982, pp. 165-172.

6. Hoh, Roger H., Thomas T. Myers, Irving L. Ashkenas, et al., Development of Handling Quality Criteria for Aircraft with Independent Control of Six Degrees of Freedom, AFWAL-TR-81-3027, Apr. 1981.

7. Allen, R. Wade, "Stability and Performance Analysis of Automobile Driver Steering Control," SAE Paper 820303, presented at the 1982 SAE International Annual Congress and Exposition, Detroit, MI, 22-26 Feb. 1982.

8. Hodgkinson, J., W. J. LaManna, and J. L. Heyde, "Handling Qualities of Aircraft with Stability and Control Augmentation Systems -- a Fundamental Approach," Aeronautical Journal, Vol. 80, No. 782, Feb. 1976, pp. 75-81.

9. McRuer, Duane T., and Richard H. Klein, "Comparison of Human Driver Dynamics in an Automobile on the Road with Those in Simulators Having Complex and Simple Visual Displays," Systems Technology, Inc., P-173A, presented at the 55th Annual Meeting of the Transportation Research Board, Washington, D.C., 19-23 Jan. 1976.

10. Gum, D. R., and W. B. Albery, "Time-Delay Problems Encountered in Integrating the Advanced Simulator for Undergraduate Pilot Training," J. Aircraft, Vol. 14, No. 4, Apr. 1977, pp. 327-332.

11. Allen, R. Wade, "Modeling Driver Steering Control Behavior," Systems Technology, Inc., P-322, presented at the 1982 IEEE International Conference on Cybernetics and Society, Seattle, WA, 28-30 Oct. 1982.

12. Allen, R. Wade, and Henry R. Jex, "Driving Simulation -- Requirements, Mechanization and Application," SAE Paper 800448, presented at the SAE Congress and Exposition, Detroit, MI, Feb. 1980; also SAE Trans., Vol. 89, 1981, pp. 1769-1780.

13. Howe, R. M., "Special Considerations in Real-Time Digital Simulation," The Proceedings of the 1983 Summer Computer Simulation Conference, Volume 1, 11-13 July 1983, Vancouver, B.C., Canada.